Analyst

PAPER

View Article Online
View Journal

Cite this: DOI: 10.1039/c4an02010c

A human telomeric G-quadruplex-based electronic nanoswitch for the detection of anticancer drugs†

Zahra Bagheryan,[a] Jahan-Bakhsh Raoof,*[a] Reza Ojani[a] and Parizad Rezaei[b]

Received 2nd November 2014,
Accepted 30th March 2015

DOI: 10.1039/c4an02010c

www.rsc.org/analyst

An electronic nanoswitch is described based on the conformational change of the DNA sequence in the presence of stabilizing ligands. The new electrochemical biosensor was prepared by modifying a screen-printed graphite electrode (SPE) with functionalized SiO_2 nanoparticles [(SiO_2-*N*-propylpiperazine-*N*-(2-mercaptopropane-1-one) (SiO_2@NPPNSH)] and Au nanoparticles (AuNPs). These nanoparticles are able to immobilize thiolated G-quadruplex DNA structures (SH-G_4DNA). The SH groups on the SiO_2@NPPNSH nanoparticles provide a good platform for stabilizing AuNPs on the surface of the electrode. This is due to the fact that AuNPs are able to bind to the organic SH groups on the SiO_2@NPPNSH. The SH-G_4DNA binds to the modified electrode by a AuNPs–S bond. The structure of SiO_2@NPPNSH was characterized by scanning electron microscopy (SEM), thermo-gravimetric analysis (TGA) and infrared (IR) spectroscopy. The morphology of the modified electrode was characterized by SEM. The interaction between G_4DNA and the anticancer drug, Tamoxifen (Tam), was studied in Tris–HCl buffer and $[Fe(CN)_6]^{3-}$ using cyclic (CV) and square wave voltammetry (SWV). The G-quadruplex formation and the interaction mechanism were identified by circular dichroism (CD) measurements. The CV current was seen to decrease with increasing concentration of Tam due to interaction between G_4DNA and Tam. This biosensor is a simple and useful tool for selecting G-quadruplex-binding ligands.

1. Introduction

The specialized nucleoprotein structures at the end of linear chromosomes are known as telomeres. These structures become shorter due to cell division, and this can be a risk factor in the development of cancer.[1–3] The enzyme telomerase maintains the length of the telomeres, enabling cells to replicate their telomeric sequences during cell division.[4] Human telomeres are composed of tandem repeats of the double-stranded DNA sequence, (5-TTAGGG):(5-CCCTAA). The G-rich strand can form G-quadruplex structures *via* the Hoogsteen base pair.[5] The strand also can be stabilized by monovalent cations such as K^+ and Na^+.[6] According to a number of studies, G-quadruplex structures in certain regions of the genome may play a role in the poor maintenance of genomic stability, which is a characteristic of many DNA repair disorders and some types of cancer.[7,8] In addition, telomerase is activated in 90% of cancer cells.[3]

Based on a number of earlier reports, the formation and stabilization of quadruplex structures at the telomeric repeats is an effective method of inhibiting telomerase activity. These processes hamper telomere extension, blocking the elongation step.[9] Small molecules able to target the G-quadruplex through a variety of binding modes have aroused considerable interest during studies of these molecules, due to their potential clinical application in the diagnosis of diseases and the design of drugs,[10–12] particularly in the development of anticancer therapies.[1] For instance, appropriate ligands with a good affinity for G-quadruplex structures can be used to stabilize or fold this DNA structure in cancer therapy.

Tamoxifen (Tam) is an anti-estrogen, introduced in 1970. It has become one of the most popular hormonal agents for the treatment of breast cancer in women.[13–15] Tam belongs to a class of drugs known as *selective estrogen receptor modulators*, and was one of the earliest medications employed for targeted therapies in breast cancer.[16]

In continuation of our previous studies on the electrochemical features of G_4DNA–ligand interaction,[17,18] in the present paper we describe a new nanobiosensor, constructed using G-quadruplex, for the electrochemical investigation of a

[a]*Electroanalytical Chemistry Research Laboratory, Department of Analytical Chemistry, Faculty of Chemistry, University of Mazandaran, Babolsar, Iran. E-mail: j.raoof@umz.ac.ir; Fax: +98-11-35302350; Tel: +98-11-35302392*
[b]*Department of Chemical Engineering, Islamic Azad University, Abadan Branch, Abadan, Iran*

†Electronic supplementary information (ESI) available. See DOI: 10.1039/c4an02010c

number of ligands able to stabilize this structure. A graphite screen-printed electrode (SPE), which is low in cost and mass-producible,[19,20] was modified with functionalized SiO_2 nanoparticles (SiO_2@NPPNSH), and AuNPs were then introduced to the electrode surface, and the organic SH groups on SiO_2@NPPNSH were able to bind to the AuNPs on the electrode surface. SH-G_4DNA could then link to the modified electrode by a AuNPs–S bond. The resulting nanobiosensor could then form a substrate for investigating G_4DNA-binding ligands on the electrode surface. Tam was selected as a G-quadruplex-binding model ligand and its affinity towards G_4DNA was examined. The G-quadruplex formation and also the interaction between G_4DNA and Tam were investigated by electrochemical signal change and by circular dichroism (CD) spectroscopy.

2. Experimental

2.1 Reagents

Nanosilica (12.6 nm average particle size) was purchased from Nissan Chemical Industries Ltd, Tokyo. The DNA oligonucleotides were purchased from MWG-Biotech, Ebersberg, Germany, and had the following base sequences:

Single-stranded human telomeric DNA (ssDNA):

Sequence 1: (5′ GGG TTA GGG TTA GGG TTA GGG 3′)

Sequence 2: (SH-5′ GGG TTA GGG TTA GGG TTA GGG 3′)

Complementary oligonucleotide: (5′ CCC TAA CCC TAA CCC TAA CCC 3′)

Sequence 1 was used for experiments carried out in solution and Sequence 2 to prepare the mixed self-assembled monolayers. All other materials and reagents were supplied commercially by either Aldrich or Merck.

A stock solution of DNA (1.0 μM) was prepared in deionized water (50 mM Tris–HCl, 1.0 mM EDTA, pH 8.00) and held at 4 °C for future use. A stock solution of the G-quadruplex structure of human telomeric DNA (G_4DNA) was obtained by adding 100 mM KCl and 1.0 μM ssDNA, and the solution was held at 4 °C for 20 min; the solution containing ssDNA and its complementary sequences and 100 mM KCl was heated at 95 °C for 10 min and then slowly allowed to cool to room temperature to form double-stranded DNA (dsDNA).[21] The supporting electrolyte used in all experiments was 50 mM Tris–HCl buffer at pH 7.40.

2.2 Instrumentation

Electrochemical studies were performed using a Metrohm Autolab PG 30 electrochemical analysis system controlled by GPES 4.9 and FRA software (Eco Chemie, Netherlands). The screen-printed electrodes (SPE, Florence, Italy) were made up of a carbon working electrode, a carbon counter-electrode and a silver pseudo-reference electrode. The materials and procedures for screen printing the transducers have been described elsewhere.[22] CD spectra were measured using a Model 215 CD spectrometer (Aviv, USA) between 320 and 200 nm. Standard quartz cells of 1 cm path length were used for all CD experiments. Circular dichroism nerve network software was used for data analysis. All the experiments were carried out at room temperature. The structure of SiO_2@NPPNSH at each step of electrode modification was investigated using a SEM (Cambridge Stereo Scan 360) system. Thermo-gravimetric analysis (TGA) was conducted on a Stanton Redcraft STA-780 (London) and IR spectra were determined on a Bruker instrument.

2.3 Procedure

2.3.1 Preparation of SiO_2-*N*-propylpiperazine-*N*-(2-mercaptopropane-1-one). Functionalized SiO_2 nanoparticles (SiO_2NPs) were prepared according to the typical heterogeneous process (Scheme 1). SiO_2NPs (2.0 g) was first refluxed with 3-chloropropyltrimethoxysilane (3.0 mL) in dry toluene (100 mL) for 24 h. A suspension of SiO_2NPs@Cl (1 g) in 100 cm^3 of xylene was then added to piperazine (0.5 g) in the presence of triethylamine (1 mL) with continuous stirring under a nitrogen atmosphere for 48 h at 70 °C. The product (SiO_2NPs@Py) was filtered off and washed with xylene and hot ethanol for 12 h in a continuous Soxhlet extractor, then dried under vacuum. A magnetically stirred mixture of SiO_2NPs@Py (1.0 g) was refluxed with 2-mercaptopropanoic acid (1 mL) in toluene for 24 h and the product filtered off using a sintered glass funnel. The mixture was washed with hot toluene for 12 h in a continuous Soxhlet extractor, followed by overnight drying in an oven at 110 °C, to give silica-bonded-*N*-propylpiperazine-*N*-(2-mercaptopropane-1-one) (SiO_2@NPPNSH).

2.3.2 Preparation of a modified SPE for the investigation of G_4DNA/ligand interaction. A droplet of 10 μL SiO_2@NPPNSH was placed on the working electrode surface and air dried for 1.0 h. It was then soaked in ultrapure water to remove unabsorbed SiO_2@NPPNSH. Absorption of AuNPs was carried out in an aqueous solution of 0.5 mM $HAuCl_4$ using chronoamperometry. The electrode potential was stepped down from −0.23 V, with a deposition time of 300 s. Following these pretreatments 10 μL of 1 μM G_4DNA solution was added to the modified SPE, after which incubation was carried out at room temperature for 3 h. Next, mercaptoethanol (10 μL) was added to the modified G_4DNA/AuNPs/SiO_2/SPE, and the electrode finally rinsed with ultrapure water. The interaction of G_4DNA and ligands on the working electrode surface was assessed by immersing the G_4DNA/AuNPs/SiO_2/SPE in ligand solution, 15 min being chosen as the optimal time for G_4DNA/Tam interaction. Scheme 1 describes the formation of the biosensing platform for selecting G_4DNA ligands.

3. Results and discussion

3.1 Characterization of functionalized SiO_2 nanoparticles (SiO_2@NPPNSH)

The SiO_2@NPPNSH were first characterized by SEM, as shown in Fig. 1(A). Comparison of the primary particles and the final nanoparticles showed that the latter were approximately 30–40 nm in size, and that they exhibited some degree of

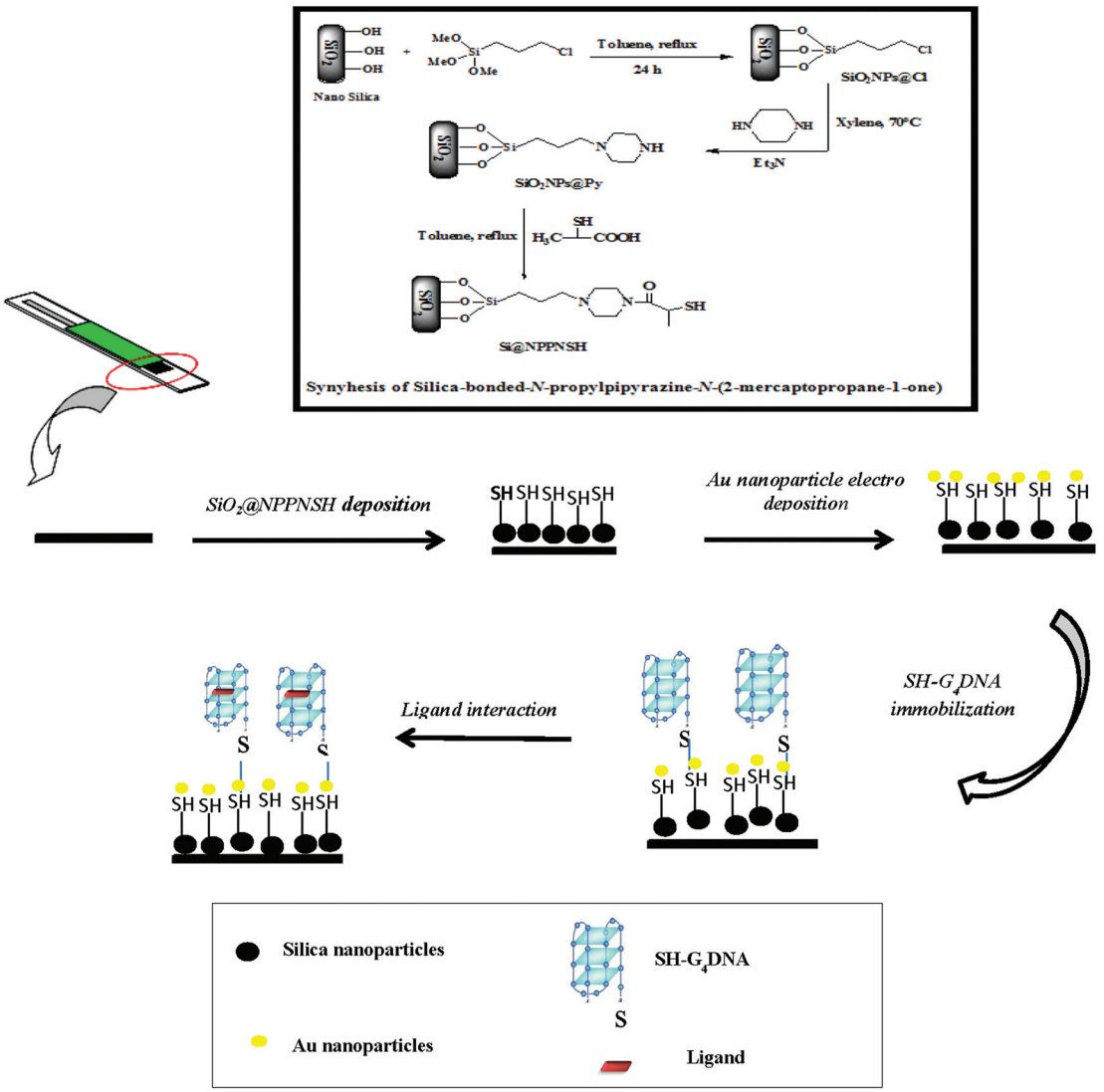

Scheme 1 Schematic diagram showing preparation of the modified electrode.

aggregation. The chemical structure of SiO_2@NPPNSH was confirmed by Fourier–transform infrared (FT-IR) spectrometry and TGA. A number of characteristic peaks in the FT-IR spectra around 3500–3300, 2933, 2553, 1660–1550 and 1250–1040 cm^{-1} were due to the O–H of silanols, C–H, SH and Si–O–Si stretching vibrations, and overlapping free OH and C═O groups, respectively, confirming the presence of organic functional groups in the SiO_2@NPPNSH framework (Fig. 1(B)).

The amount of grafted organic species was determined by TGA (Fig. 1(C)). The loading of *ca.* 0.88 mmol g^{-1} for a surface-bound group was in good agreement with the result obtained by elemental analysis. The quantity of mercapto groups attached to SiO_2NPs estimated from the sulfur percentage (2.72%) by elemental analysis was 0.85 mmol g^{-1}.

3.2 Modification of the electrode

Fig. 2 illustrates SEM images of modified SPEs, Fig. 2(A) showing the bare SPE. Fig. 2(B) shows the SiO_2@NPPNSH nanoparticles after deposition on the SPE, and Fig. 2(C) the morphology of SiO_2@NPPNSH/SPE after AuNPs electro-deposition. AuNPs were attached to the SiO_2@NPPNSH by a S–Au bond. The thiolated functionalized group on the SiO_2@NPPNSH assisted the deposition of AuNPs, and also stabilized the AuNPs on the surface of the electrode.

3.3 Characterization by CD spectroscopy of the G_4DNA formed in solution

Circular dichroism (CD) spectra can be a suitable method for identifying the G-quadruplex structure and identifying the differences between dsDNA and the secondary structure of single-stranded DNA such as G-quadruplex and I-motif. To confirm whether the G-quadruplex structure had formed in solution, CD experiments were performed before any attempt was made to immobilize the G_4DNA on the surface of the modified electrodes. The human telomeric sequence can exist as a parallel structure (a positive band around 265 nm and a

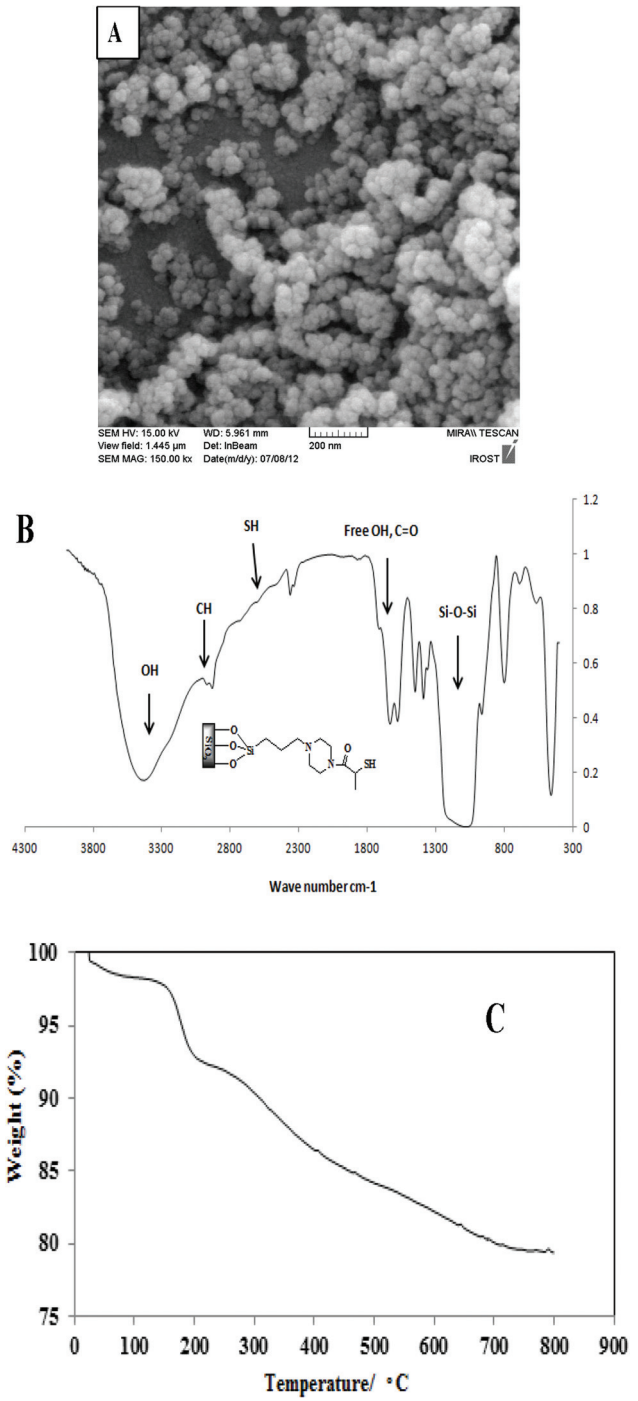

Fig. 1 (A) SEM image of the compound SiO_2@NPPNSH. (B) FT–IR spectra of SiO_2@NPPNSH. (C) TGA analysis of SiO_2@NPPNSH.

negative band around 240 nm),[23] an anti-parallel structure (a positive band around 295 nm and a negative band around 260 nm),[24] or a combination of the two.[25] The dsDNA structure showed a positive peak at 260 nm.[26] As can be seen in Fig. 3(A) (curve (a)), the CD spectrum of the G_4DNA showed a positive band around 265 nm and a negative band around 240 nm, confirming the parallel structure.

It was observed that the spectra of G_4DNA in the presence of different Tam concentrations exhibited a dramatic increase in the negative band at 240 nm and a decrease in the positive band at 260 nm (curves (b) and (c)). To further assess the interaction, control experiments were conducted with ssDNA before adding KCl, in order to change the structure of the human telomeric DNA and ultimately generate G_4DNA. As Fig. 3(B) demonstrates, the CD spectrum of the ssDNA showed a positive band at about 260 nm (curve (a)). In the presence of Tam, the spectra exhibited a dramatic increase in the negative band at 240 nm and a decrease in the positive band at 260 nm, related to the parallel type of structure. The CD spectra suggested that Tam interacted strongly with the G_4DNA and that it could stabilize the G-quadruplex structure, even in the absence of stabilizing cations.

3.4 Electrochemical behavior of the proposed biosensor using $[Fe(CN)_6]^{3-}$ as a redox label

To demonstrate that the G_4DNA had been immobilized on the modified electrode surface, CV signals were performed in 50 mmol L^{-1} Tris–HCl buffer solutions (pH 7.40) containing 0.01 mol L^{-1} $[Fe(CN)_6]^{3-}$ and 100 mmol L^{-1} KCl, at scan rate of 50 mV s^{-1} (Fig. 4(A)). In the CV measurements, the peak current increased after modifying the SPE with SiO_2@NPPNSH (curve (b)) and AuNPs (curve (c)), respectively, compared with the result of the bare electrode (curve (a)). Indeed, SiO_2@NPPNSH and AuNPs can significantly enhance the electron transfer as mediator, due to their vast surface area. When the modified electrode was immobilized with G_4DNA, the CV signal decreased, and its ΔE_p increased due to the increase in surface charge density (curve (d)). The electrostatic repulsive interactions between the G_4DNA negative backbone and $[Fe(CN)_6]^{3-}$ had a decreasing effect on the redox signal, indicating that a compactly packed self-assembled monolayer of thiolated G_4DNA and MCH had formed.

The quality of G_4DNA immobilization on the electrode surface was compared with an electrode modified by the absence of SiO_2@NPPNSH (ESI Fig. S1†). The presence of SiO_2@NPPNSH improved the electrodeposition of AuNPs on the electrode surface. The SH organic group on the SiO_2 gave an increase in AuNP electrodeposition. This group also increased the $[Fe(CN)_6]^{3-}$ redox signal (curve (b)) compared with the effect of the AuNP-modified electrode in the absence of SiO_2@NPPNSH (curve (a)). As a result, G_4DNA immobilization was better on AuNPs/SiO_2@NPPNSH/SPE (curve (c)), compared with the effect of AuNPs/SPE (curve (d)).

In the next phase of the study, the electrochemical response of the G_4DNA/AuNPs/SiO_2@NPPNSH/SPE was investigated in the presence of Tam in $[Fe(CN)_6]^{3-}$ solution (ESI Fig. S2†). As increasing concentrations of Tam were added to the solution the CV peak current gradually decreased, demonstrating specific interaction between G_4DNA and Tam. On the assumption that G_4DNA and the ligand (L) produced only a single complex (eqn (1)):

$$G_4DNA + mL \rightarrow G_4DNA\text{–}L_m, \quad (1)$$

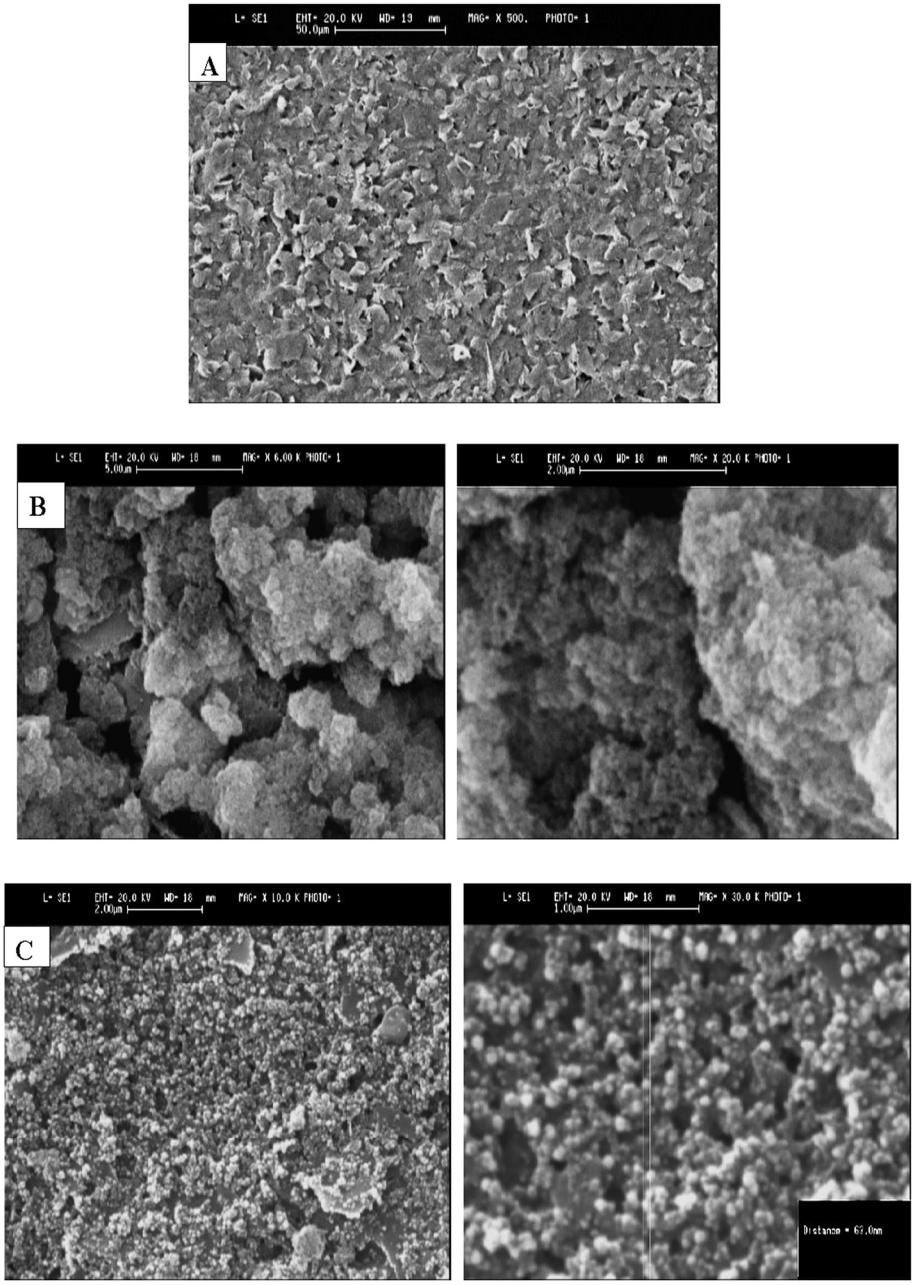

Fig. 2 SEM images of (A) bare SPE, (B) SiO_2@NPPNSH/SPE, and (C) AuNPs/SiO_2@NPPNSH/SPE.

The binding constant (K_b) can be detected, based on eqn (2), as described by Ibrahim.[27] The modified equation in the literature[28] was used, with minor modification. K_b can be deduced as follows (eqn (2)):

$$\log \frac{I_{DNA-L}}{I_{DNA} - I_{DNA-L}} = -\log K_b + m \log \frac{1}{[L]} \quad (2)$$

In this equation, K_b is the apparent binding constant, I_{DNA} the peak current of immobilized G_4DNA alone, L is the ligand (Tam), and I_{DNA-L} the peak current of G_4DNA after interaction with Tam. If G_4DNA and the ligand form a single complex, the plot of $(I_{DNA-L}/(I_{DNA}-I_{DNA-L}))$ *vs.* $\log\left(\frac{1}{[L]}\right)$ becomes linear, with slope m and intercept K_b. According to eqn (1), a plot of $\log(I_{DNA-L}/(I_{DNA}-I_{DNA-L}))$ against log (1/[L]) results in a straight line (Fig. 4(B)). The K_b value was deduced from the intercept value of the linear plot, arriving at a value for K_b of 5.74×10^5 mol L^{-1}.

3.5 Voltammetric evaluation of Tam–G_4DNA interaction

In order to investigate the mechanism of the interaction of Tam with G_4DNA, an electrochemical study was performed using cyclic voltammetry under G_4DNA/AuNPs/

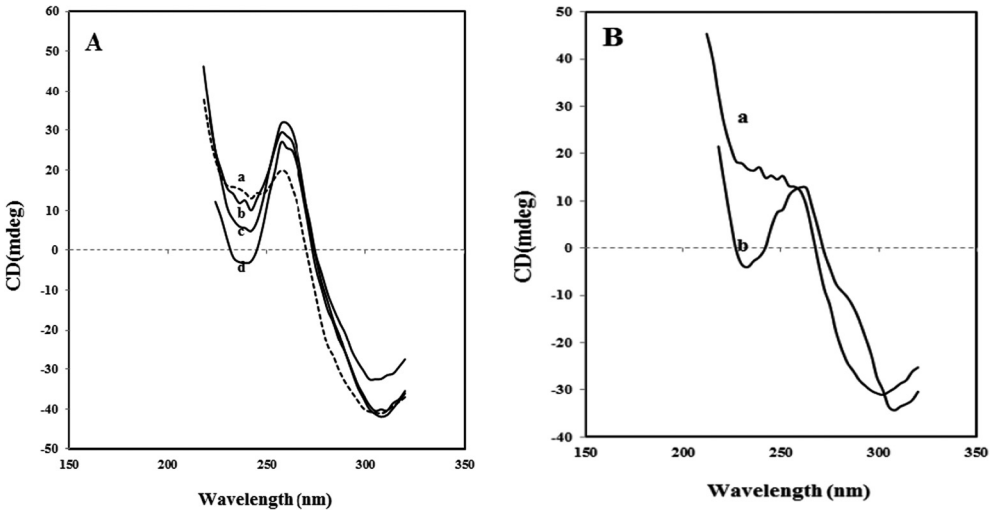

Fig. 3 CD spectrum of (A) 1.0 μmol L^{-1} G_4DNA (a) in the absence and the presence of different concentrations of Tam: (b) 1.0 × 10^{-7} mol L^{-1}, (c) 1.0 × 10^{-6} mol L^{-1}, and (d) 1.0 × 10^{-5} mol L^{-1}. (B) 1.0 μmol L^{-1} ssDNA (a) in the absence and (b) the presence of: 1.0 × 10^{-6} mol L^{-1} Tam.

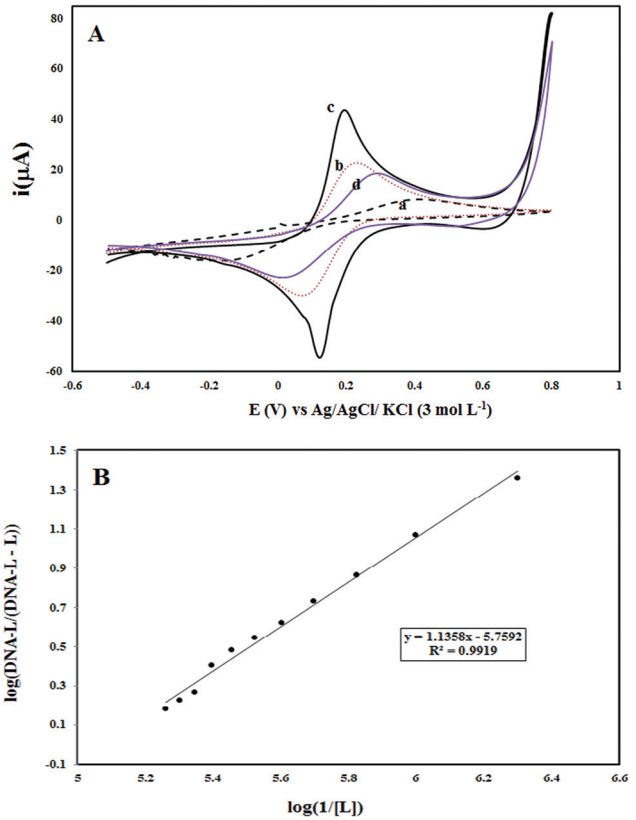

Fig. 4 (A) Cyclic voltammograms of (a) SPE, (b) SiO_2@NPPNSH/SPE, (c) AuNPs/SiO_2@NPPNSH/SPE and G_4DNA/AuNPs/SiO_2@NPPNSH/SPE in 0.5 mmol L^{-1} $[Fe(CN)_6]^{3-}$ and 100 mmol L^{-1} KCl, at a scan rate of 50 mV s^{-1}. (B) Plot of $\log(I_{DNA-L}/I_{DNA} - I_{DNA-L})$ *vs.* log(1/[L]) for determination of the binding constant.

SiO_2@NPPNSH/SPE conditions. Cyclic voltammograms at 1.0 × 10^{-4} mol L^{-1} Tam showed only one oxidation peak, at E_{pa} = +0.85–0.90 V (Fig. 5(A)), associated with oxidation of the Tam. It can be seen that the peak current of Tam increased (b) after addition of SiO_2@NPPNSH, (c) after AuNP deposition, and (d) after G_4DNA immobilization, respectively, compared with the bare electrode (a), and there was also a shift in the oxidation peak to a lower positive potential. It is clear that the SH groups of SiO_2@NPPNSH caused a preconcentration of AuNPs on the surface of the working electrode. Thereafter, SH-G_4DNA became linked to the AuNPs, which were bonded to the s-functionalized group of SiO_2@NPPNSH. In the presence of Tam, the interaction of Tam/G_4DNA took place on this platform. It is clear that the oxidation peak current of Tam increased following interaction with G_4DNA.

Square wave voltammetry (SWV) was employed to ensure G_4DNA immobilization. Immobilization on the electrode surface was evaluated by SW measurement in 50 mM Tris–HCl buffer solution (pH 7.40). To investigate the interaction of G_4DNA with Tam on the working electrode surface, G_4DNA immobilized at the modified SPE, and then the immobilized G_4DNA modified SPE, were immersed in ligand solution for 15 min without applying a potential at the working electrode. The electrode was then carefully rinsed with distilled water and SW voltammograms were recorded between +0.5 and +1.3 V *vs.* Ag/AgCl/KCl (3 M) in Tris–HCl buffer (50 mM Tris–HCl buffer, 100 mM KCl, pH 7.40).

Fig. 5(B) shows square wave voltammograms for (a) bare SPE, (b) SiO_2@NPPNSH/SPE, (c) AuNPs/SiO_2@NPPNSH/SPE, (d) SH-G_4DNA/AuNPs/SiO_2@NPPNSH/SPE, (e) 1 × 10^{-7} mol L^{-1} Tam/SH-G_4DNA/AuNPs/SiO_2@NPPNSH/SPE, (f) 1 × 10^{-6} mol L^{-1} Tam/SH-G_4DNA/AuNPs/SiO_2@NPPNSH/SPE and (g) 1 × 10^{-5} mol L^{-1} Tam/SH-G_4DNA/AuNPs/SiO_2@NPPNSH/SPE. SW voltammograms obtained immediately after G_4DNA deposition on the modified electrode surface showed an increase in the intensity of the Tam oxidation peaks.

These results demonstrated that Tam can intercalate into the G_4DNA structure; its oxidation signal can be seen following

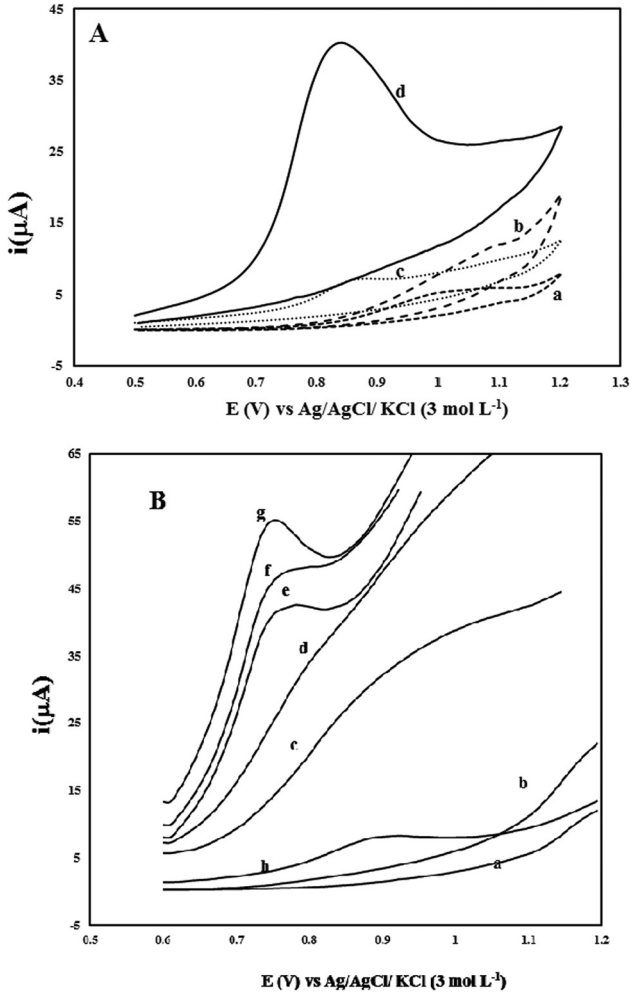

Fig. 5 (A) (a) CV signals of 1×10^{-4} mol L^{-1} Tam in a 50 mmol L^{-1} Tris–HCl solution at the SPE, (b) SiO_2@NPPNSH/SPE, (c) AuNPs/SiO_2@NPPNSH/SPE and (d) G_4DNA/AuNPs/SiO_2@NPPNSH/SPE at a scan rate of 50 mV s^{-1}. (B) SW voltammograms of (a) SPE, (b) SiO_2@NPPNSH/SPE, (c) AuNPs/SiO_2@NPPNSH/SPE, (d) G_4DNA/AuNPs/SiO_2@NPPNSH/SPE, (e) 1×10^{-7} mol L^{-1} Tam/G_4DNA/AuNPs/SiO_2@NPPNSH/SPE, (f) 1×10^{-6} mol L^{-1} Tam/G_4DNA/AuNPs/SiO_2@NPPNSH/SPE, (g) 1×10^{-4} mol L^{-1} Tam/G_4DNA/AuNPs/SiO_2@NPPNSH/SPE and (h) 1×10^{-6} mol L^{-1} Tam /AuNPs/SiO_2@NPPNSH/SPE in a 50 mmol L^{-1} Tris–HCl solution.

Table 1 DNA probe for selectivity study

DNA molecules	Structure
dsDNA(I)	SH-GGG TTA GGG TTA GGG TTA GGG CCC AAT CCC
dsDNA(II)	SH-GGG TTA GGG TTA GGG TTA GGG CCC AAT CCC AAT
dsDNA(III)	SH-GGG TTA GGG TTA GGG TTA GGG CCC AAT CCC AAT CCC
dsDNA(IV)	SH-GGG TTA GGG TTA GGG TTA GGG CCC AAT CCC AAT CCC AAT
ssDNA	SH-GGG TTA GGG TTA GGG TTA GGG

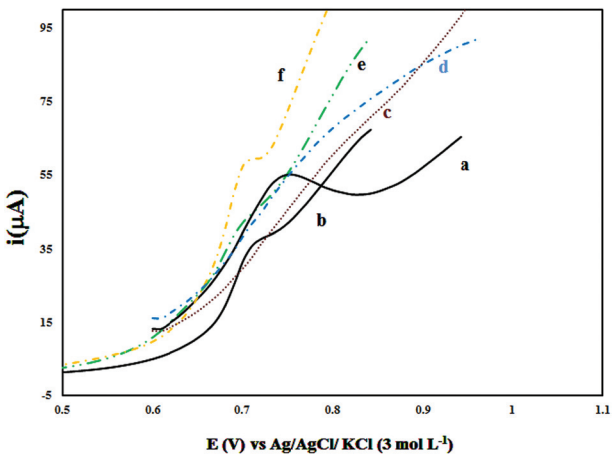

Fig. 6 SWV signals of (a) 1×10^{-5} M Tam in G_4DNA/AuNPs/SiO_2@NPPNSH/SPE, (b) dsDNA(I)/AuNPs/SiO_2@NPPNSH/SPE, (c) dsDNA (II)/AuNPs/SiO_2@NPPNSH/SPE, (d) dsDNA(III)/AuNPs/SiO_2@NPPNSH/SPE, (e) dsDNA(IV)/AuNPs/SiO_2@NPPNSH/SPE and (f) ssDNA/AuNPs/SBA@NPPNSH/SPE in Tris–HCl buffer solution (pH 7.40) at the surface of the electrode.

G_4DNA immobilization. The oxidation signals of Tam increased as its concentration increased (curves (e)–(g)). Moreover, the absence of the Tam oxidation peak in the absence of G_4DNA (curve (h)) confirmed that the appearance of Tam oxidation peaks was indeed the result of intercalation to the G_4DNA structure, and was not due to blocking of the electrode surface.

In the next step, the biosensor was also treated with a number of different dsDNA oligonucleotides (Table 1) and G_4DNA (Fig. 6). The modified electrodes were then immersed in 1.0×10^{-5} M Tam solution and the SWV recorded. As can be seen, the interaction between Tam and different dsDNA and ssDNA molecules did not give a significant increase in the SW signals (curves (b)–(g)), in comparison to the SW signals in the presence of G_4DNA (curve (a)). A comparable SWV signal was observed in the presence of dsDNA(I) (curve (b)), since in this situation the complementary strand was small and G_4DNA can be formed after the Tam addition. In the other situation, the complementary strand was bigger and G_4DNA could not be produced, and Tam could therefore not intercalate into the structure, and no oxidation signal was observed (curves (c)–(e)). In the presence of ssDNA the G_4DNA could not be stabilized in the absence of KCl, and only a small signal was therefore observed after Tam addition (curve (f)).

4. Conclusions

A AuNPs/SiO_2@NPPNSH-modified graphite SPE was employed to study the interaction between Tam and G_4DNA. The experi-

mental results confirmed that this platform offered a simple, relevant and effective surface area for selecting ligands which were able to interact with the G-quadruplex structure. The voltammetric results showed that SiO_2@NPPNSH could stabilize AuNPs on the electrode and thus increase G_4DNA immobilization. The G_4DNA/Tam interaction was studied using CV and SWV at modified SPE. CD spectroscopy was employed to confirm the formation of G_4DNA in solution. Data from the voltammetric studies and CD spectroscopy indicated that Tam was able to interact with the G_4DNA structure and increase its stability. The nanostructured G_4DNA electrochemical biosensor will be useful for selecting the G-quadruplex-binding ligand at physiological pH. Reports from our laboratory are in hand regarding the application of the electronic nanoswitch for assessing the antitumor activity of ligands and drugs.

References

1 S. Neidle and G. Parkinson, *Nat. Rev. Drug Discovery*, 2002, **1**, 383–393.
2 D. Sun, B. Thompson, B. E. Cathers, M. Salazar, S. M. Kerwin, J. O. Trent, T. C. Jenkins, S. Neidle and L. H. Hurley, *J. Med. Chem.*, 1997, **40**, 2113–2116.
3 S. Cogoi, M. Paramasivam, B. Spolaore and L. E. Xodo, *Nucleic Acids Res.*, 2008, **36**, 3765–3780.
4 C. W. Greider, *Proc. Natl. Acad. Sci. U. S. A.*, 1998, **95**, 90–92.
5 J. T. Davis, *Angew. Chem., Int. Ed.*, 2004, **43**, 668–698.
6 Y. Wu and R. M. Brosh, *FEBS J.*, 2010, **277**, 3470–3488.
7 M. Paramasivam, A. Membrino, S. Cogoi, H. Fukuda, H. Nakagama and L. E. Xodo, *Nucleic Acids Res.*, 2009, **37**, 2841–2853.
8 S. Cogoi and L. E. Xodo, *Nucleic Acids Res.*, 2006, **34**, 2536–2549.
9 Y. Mikami-Terao, M. Akiyama, Y. Yuza, T. Yanagisawa, O. Yamada and H. Yamada, *Cancer Lett.*, 2008, **261**, 226–234.
10 T.-m. Ou, Y.-j. Lu, J.-h. Tan, Z.-s. Huang, K.-Y. Wong and L.-q. Gu, *ChemMedChem*, 2008, **3**, 690–713.
11 J. E. Reed, A. A. Arnal, S. Neidle and R. Vilar, *J. Am. Chem. Soc.*, 2006, **128**, 5992–5993.
12 P. V. Jena, P. S. Shirude, B. Okumus, K. Laxmi-Reddy, F. Godde, I. Huc, S. Balasubramanian and T. Ha, *J. Am. Chem. Soc.*, 2009, **131**, 12522–12523.
13 R. E. McDaniel, P. Y. Maximov and V. C. Jordan, in *Vitamins & Hormones*, ed. L. Gerald, Academic Press, 2013, vol. 93, pp. 1–49.
14 J. M. P. J. Garrido, E. Manuela, P. J. Garrido, A. Maria Oliveira-Brett and F. Borges, *Curr. Drug Metab.*, 2011, **12**, 372–382.
15 V. C. Jordan, *Nat. Rev. Drug Discovery*, 2003, **2**, 205–213.
16 P. Bourassa, T. J. Thomas and H. A. Tajmir-Riahi, *J. Pharm. Biomed. Anal.*, 2014, **95**, 193–199.
17 Z. Bagheryan, J.-B. Raoof, R. Ojani and P. Rezaei, *Talanta*, 2014, **119**, 24–33.
18 Z. Bagheryan, J.-B. Raoof, R. Ojani and E. Hamidi-Asl, *Electroanalysis*, 2013, **25**, 2659–2667.
19 R. O. Kadara, N. Jenkinson and C. E. Banks, *Sens. Actuators, B*, 2009, **138**, 556–562.
20 M. Tudorache and C. Bala, *Anal. Bioanal. Chem.*, 2007, **388**, 565–578.
21 J. Ruiz-Chica, M. A. Medina, F. Sánchez-Jiménez and F. J. Ramírez, *Biochim. Biophys. Acta, Gene Struct. Expression*, 2003, **1628**, 11–21.
22 S. Laschi, I. Palchetti, G. Marrazza and M. Mascini, *J. Electroanal. Chem.*, 2006, **593**, 211–218.
23 G. N. Parkinson, M. P. H. Lee and S. Neidle, *Nature*, 2002, **417**, 876–880.
24 Y. Wang and D. J. Patel, *Structure*, 1993, **1**, 263–282.
25 A. Ambrus, D. Chen, J. Dai, T. Bialis, R. A. Jones and D. Yang, *Nucleic Acids Res.*, 2006, **34**, 2723–2735.
26 W. Li, D. Miyoshi, S.-i. Nakano and N. Sugimoto, *Biochemistry*, 2003, **42**, 11736–11744.
27 M. S. Ibrahim, *Anal. Chim. Acta*, 2001, **443**, 63–72.
28 L. Wang, L. Lin and B. Ye, *J. Pharm. Biomed. Anal.*, 2006, **42**, 625–629.

